Liquid Crystals
Publication details, including instructions for authors and subscription information:
http://www.informaworld.com/smpp/title~content=t713926090

Elastic constant anisotropy and disclination interaction in nematic polymers II. Effect of disclination interaction

Wenhui Song; Houjie Tu; Gerhard Goldbeck-wood; Alan H. Windle Corresponding author

Online publication date: 19 May 2010

To cite this Article Song, Wenhui , Tu, Houjie , Goldbeck-wood, Gerhard and Windle Corresponding author, Alan H.(2003) 'Elastic constant anisotropy and disclination interaction in nematic polymers II. Effect of disclination interaction', Liquid Crystals, 30: 7, 775 — 784

To link to this Article: DOI: 10.1080/0267829031000111441

URL: http://dx.doi.org/10.1080/0267829031000111441

LIQUID CRYSTALS, VOL. 30, NO. 7, JULY, 2003, 775–784

Elastic constant anisotropy and disclination interaction in nematic polymers II. Effect of disclination interaction

WENHUI SONG, HOUJIE TU, GERHARD GOLDBECK-WOOD and ALAN H WINDLE*

Department of Materials Science and Metallurgy, Cambridge University, Pembroke Street, Cambridge CB2 3QZ, UK

(*Received 22 August 2002; accepted 10 February 2003*)

A new tensorial approach introducing unequal elastic constants in a two-dimensional lattice model is applied to simulate the influence of disclination interaction on the structures of half-wedge disclinations, for the understanding of the variation of apparent elastic anisotropy ε_a measured from different disclinations in a texture (see preceding paper, part I [1]). The apparently random variation of ε_a implies that disclination interaction has a strong effect on the structure of disclinations; as elastic anisotropy increases, its impact becomes overpowering. Nevertheless the disclination interaction still acts in the same way as in the case of equal elastic constants. Analysis of the free energy of disclination pairs shows that the structures of both $+1/2$ and $-1/2$ disclinations are changed under the influence of a neighbouring disclination, but in different ways. For $+1/2$ disclination, the splay and bend distortions vary with the relative orientation of its $-1/2$ neighbour. Meanwhile, for $-1/2$ disclination, the bend and splay distortions are remarkably insensitive to the relative orientation of its $+1/2$ disclination neighbour.

1. Introduction

In the preceding paper part I [1], the elastic anisotropy ε of a copolyester (Cl-6) was supposed to be obtained by measuring the distortions around the $+1/2$ wedge disclinations as revealed by spontaneous band texture. However, in a given specimen, a full range of values of ε_a was obtained from the different $+1/2$ disclinations. This unexpected result reminds us that the principle on which the measurement is based assumes an ideal single disclination in the absence of any interaction with neighbouring disclinations. In reality, disclination interaction may have a significant influence on the disclination structure. The difference of the apparent elastic anisotropy in one specimen raises the basic issue of defect interaction and its impact on the structure of defects.

It is certain that disclinations with opposite sign attract and then annihilate each other. This leads to a decrease in the number of disclinations and a coarsening of the texture in the nematic state of both low molecular mass liquid crystals and liquid crystal polymers (LCPs). However, the way by which disclinations interact, and how this interaction affects the structure of individual disclinations, is little known. Ranganath [2] first considered the relative orientation of $(+1/2, -1/2)$ pairs. He proposed two types of extreme director patterns of $(+1/2, -1/2)$ pairs, with the central region rich in bend for one situation and rich in splay for the other. In his analysis, only one member of the $(+1/2, -1/2)$ pairs was energetically favoured, depending on the sign of elastic anisotropy ε. Unfortunately, few data of disclination interaction and the elastic anisotropy of materials have been presented so far, due to the limitation of current experimental techniques.

Numerical simulation provides a possible way to solve the problems beyond the experimental techniques. Much simulation work has been done to probe the microstructure and the evolution of texture in liquid crystals by using Monte Carlo algorithms to minimize the Frank elastic energy. Most of these methods have relied on the assumption of equal elastic constants. Some efforts have been made to tackle the problem in the case of different elastic constants [3–5]. Currently, a tensor model [6] has been developed to deal with the three Frank constants in nematics. A relaxation algorithm is implemented to solve the Ericksen–Leslie equation. The elastic torque is expressed by a tensorial form in order to treat the nematic symmetry. This deterministic model has been used to simulate the

*Author for correspondence;
e-mail: ahwl@cam.ac.uk

Liquid Crystals ISSN 0267-8292 print/ISSN 1366-5855 online © 2003 Taylor & Francis Ltd
http://www.tandf.co.uk/journals
DOI: 10.1080/0267829031000111441

microstructure of LCPs with and without an external field [6–8].

In this paper, the tensor model is applied in order to interpret the variation of the apparent elastic anisotropy in experimental measurements, and to find the effects of defect interaction and elastic anisotropy on the microstructure of these defects. The disclinations in the cases of unequal elastic anisotropy are quenched during the evolution from a random isotropic state with periodic boundary conditions. The apparent elastic anisotropy ε_a is measured from a few selected $+1/2$ disclinations. The energies of typical patterns of disclination pairs are analysed, and the impact of disclination interaction on the structures of wedge disclinations is discussed.

2. Tensor model

The details of the tensor model were described in [6]. In this work, a two-dimensional adaptation of the model is applied as the experimental data are from thin film specimens in which disclinations lie normal to the plane. In 2D, the Frank elastic free energy density in the vectorial form is:

$$f=\frac{1}{2}\left[k_{11}(\nabla\cdot\mathbf{n})^2+k_{33}(\mathbf{n}\times(\nabla\times\mathbf{n}))\cdot(\mathbf{n}\times(\nabla\times\mathbf{n}))\right] \quad (1)$$

which can be written in the equivalent tensorial form:

$$\begin{aligned} f=&\frac{1}{2}k_{11}\left[(n_2\nabla_1 n_1 n_1-n_1\nabla_2 n_1 n_1)^2\right.\\ &\left.+(n_2\nabla_1 n_1 n_2-n_1\nabla_2 n_1 n_2)^2\right]\\ &+\frac{1}{2}k_{33}\left[(n_1\nabla_1 n_1 n_1+n_2\nabla_2 n_1 n_1)^2\right.\\ &\left.+(n_1\nabla_1 n_1 n_2+n_2\nabla_2 n_1 n_2)^2\right] \end{aligned} \quad (2)$$

where $\mathbf{n}\cdot\mathbf{n}=1$ and k_{11} and k_{33} are the splay and the bend elastic constants, respectively. With Greek subscripts referring to the Cartesian components, $\nabla_\alpha=\partial/\partial x_\alpha$, $(x_1, x_2)=(x, y)$ in two dimensions. Equation (2) is used directly to calculate the elastic free energy of the system because nematic symmetry is conserved automatically. In the absence of an external field, the equation describing the relaxation of the director field in nematics is:

$$\frac{\partial\mathbf{n}}{\partial t}=\frac{1}{\gamma_1}(\mathbf{n}\times\mathbf{h})\times\mathbf{n} \quad (3)$$

where $\mathbf{h}$ is the 'texture field' ascribable to the spatial inhomogeneity of the directors, $\mathbf{n}\times\mathbf{h}$ is the torque per unit volume due to curvature elasticity and γ_1 is the rotational viscous coefficient. In the equilibrium state, the director $\mathbf{n}$ must orient itself parallel to the 'texture field', $\mathbf{h}$ can be expressed as [6]:

$$h_1=2n_1f_{11}+2n_2f_{12} \quad (4)$$

$$h_2=2n_1f_{12}-2n_2f_{11} \quad (5)$$

where

$$\begin{aligned} f_{11}=&k_{11}(n_2n_2\nabla_{11}n_1n_1+n_1n_1\nabla_{22}n_1n_1-2n_1n_2\nabla_{12}n_1n_1)\\ &+k_{33}(n_1n_1\nabla_{11}n_1n_1+n_2n_2\nabla_{22}n_1n_1+2n_1n_2\nabla_{12}n_1n_1)\\ &+\frac{1}{2}(k_{33}-k_{11})[(\nabla_2 n_1n_2+\nabla_1 n_1n_1)^2\\ &-(\nabla_1 n_1n_2-\nabla_2 n_1n_1)^2] \end{aligned} \quad (6)$$

$$\begin{aligned} f_{12}=&k_{11}(n_2n_2\nabla_{11}n_1n_2+n_1n_1\nabla_{22}n_1n_2-2n_1n_2\nabla_{12}n_1n_2)\\ &+k_{33}(n_1n_1\nabla_{11}n_1n_2+n_2n_2\nabla_{22}n_1n_2+2n_1n_2\nabla_{12}n_1n_2)\\ &+(k_{33}-k_{11})(\nabla_2 n_1n_2+\nabla_1 n_1n_1)(\nabla_1 n_1n_2-\nabla_2 n_1n_1) \end{aligned} \quad (7)$$

where $\nabla_{\alpha\beta}=\partial^2/\partial x_\alpha\partial x_\beta$; α, $\beta=1$, 2.

The tensor lattice model is capable of distinguishing the splay, twist and bend distortions in the three-dimensional director field. This has been tested by simulating the Fréedericksz transitions [6]. Periodic boundary conditions are used, which are correlated with the conditions during the simulation of the bulk.

3. Measurement of elastic anisotropy

Due to the great variation of the apparent elastic anisotropy in experimental measurements [1], the method for determining the intrinsic elastic anisotropy should be viewed with circumspection. The more important implication would be that the variation of ε_a obtained from different $+1/2$ disclinations in one specimen probably just reflects the complicated interaction among neighbouring disclinations. Obviously, the elastic anisotropy is not the only factor which determines the distortions surrounding $+1/2$ disclination. The disclination interaction itself may also play a role in the configurations of disclinations. From an experimental point of view, the interaction of disclinations is a difficult issue, on which numerical simulations are here brought to bear.

3.1. *Elastic Anisotropy measured from isolated disclinations*

First, only the director field of a single disclination in isolation is considered. This is a helpful comparison between ideally isolated disclinations and disclinations in polydomains in the experiments and simulations. The theoretical structures of $+1/2$ disclinations in lattices as a function of elastic anisotropy are visualized by equation (4) in [1]. Since this equation can be used only for small values of ε (theoretically, $|\varepsilon|<0.67$ [9]),

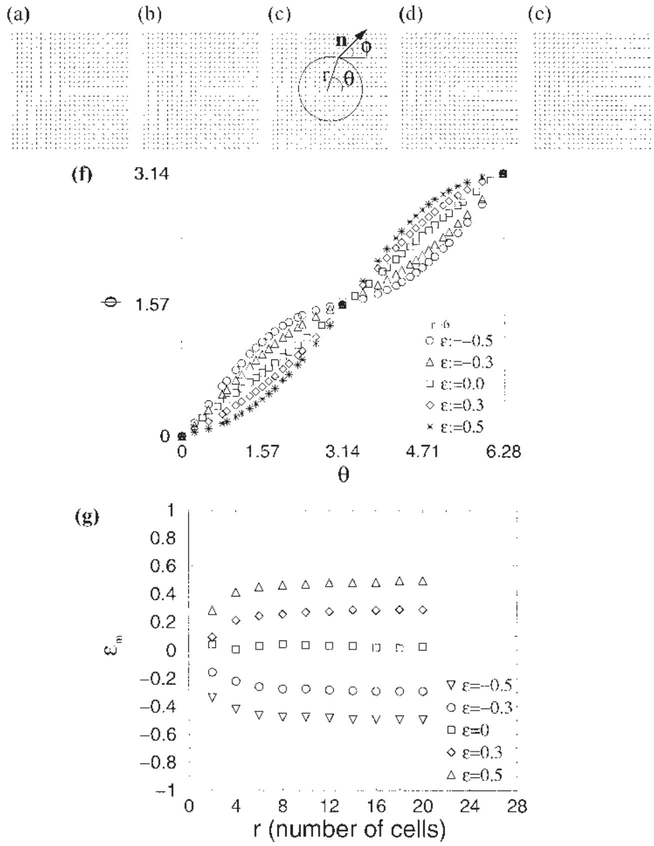

Figure 1. (*a*) Theoretical configurations for a single $+1/2$ wedge disclination dependent on elastic anisotropy ε from equation (4) in [1], after Nehring and Saupe [10]. (*a*) $\varepsilon=-0.5$; (*b*) $\varepsilon=-0.3$; (*c*) $\varepsilon=0$; (*d*) $\varepsilon=0.3$; (*e*) $\varepsilon=0.5$; (*f*) the distortion $\phi(\theta)$ data measured from single disclinations at radius $r=6$ (the number of the cells); (*g*) $\varepsilon_m(r)$ results.

figures 1 (*a–e*) show the configurations of five $+1/2$ disclinations with $\varepsilon=-0.5$, -0.3, 0, 0.3 and 0.5.

The origin of the co-ordinate system is defined at the disclination core, as shown in figure 1 (c). Hence, in the same way as in the previous work [1], the $\phi(\theta)$ data of the director field at a radius r can be determined. Figure 1 (*f*) gives five examples of $\phi(\theta)$ data measured from the disclinations in figures 1 (*a–e*) at radius $r=6$ (the number of cells) (the unit is the width of a cell). The number of data points increases with the radius. The measured elastic anisotropy, ε_m, at the different radii is determined by a least-squares fit to equation (3) in [1]. The first derivative $\partial\phi/\partial\theta$ and the second derivative $\partial^2\phi/\partial\theta^2$ can be approximated using central finite difference from the $\phi(\theta)$ data.

Figure 1 (*g*) shows the measurement results in the cases of $|\varepsilon|=0$, 0.3 and 0.5. As expected, the measured value of ε_m for each single $+1/2$ disclination matches the predefined one. Therefore, provided the disclination is in complete isolation, this numerical method can appropriately measure elastic anisotropy. The values of ε_m are consistent as the radius r increases, apart from those near the cores. The deviation of ε_m near the cores may be due to the discrete nature of the lattice. The number of available $\phi(\theta)$ data may not be enough to describe the distortions near the cores precisely, similar to those measured from the discretized director fields revealed by band texture. This issue has been discussed in detail in part I [1].

3.2. *Apparent elastic anisotropy measured from the simulated disclinations*

Microstructure formation in liquid crystalline materials is driven by the need to minimize the curvature distortions. The microstructure observed in LCPs is often far from equilibrium and unlikely to be in a minimum energy state. Hence, a model which follows the evolution of microstructure and the director field in a non-equilibrium state is appropriate for interpreting the microstructure of the materials. The defects measured in the following series of simulations are obtained by terminating simulations before all defects have been annihilated. The simulation is performed on a 100×100 lattice starting from an isotropic initial state with periodic boundary conditions.

3.2.1. *Equal elastic constants,* $k_{11}=k_{33}$

Figure 2 (*a*) is a snapshot of the director field with equal elastic constants, with four $+1/2$ disclinations highlighted. Hereafter, the core of the disclinations in the director fields is marked as a small filled box where the elastic free energy is greater than a given threshold. The disclinations in figure 2 (*a*) are quenched at 300 time steps and after a large number of disclinations have been annihilated. This means that the disclinations measured have relatively large distances between each other, which makes it easy to measure the distortions around the defects. Thus, the interaction of disclinations should be relatively small at this stage. Even so, large variations in *apparent* elastic anisotropy are observed.

The measurements of simulated disclinations are similar to experimental measurements described in [1]. Figures 2 (*b*) and 2 (*c*) give the measurement results of the four $+1/2$ disclinations selected in figure 2 (*a*). Again, the apparent value of ε_a has a near constant value over a considerable radius range from the selected disclination core. The $\phi(\theta)$ data measured from them show different distortions in figure 2 (*b*). The distortions of the $+1/2$ disclinations vary from the predominant splay to the predominant bend for disclinations A to D. In fact, the $\phi(\theta)$ data in figure 2 (*b*) are no longer as

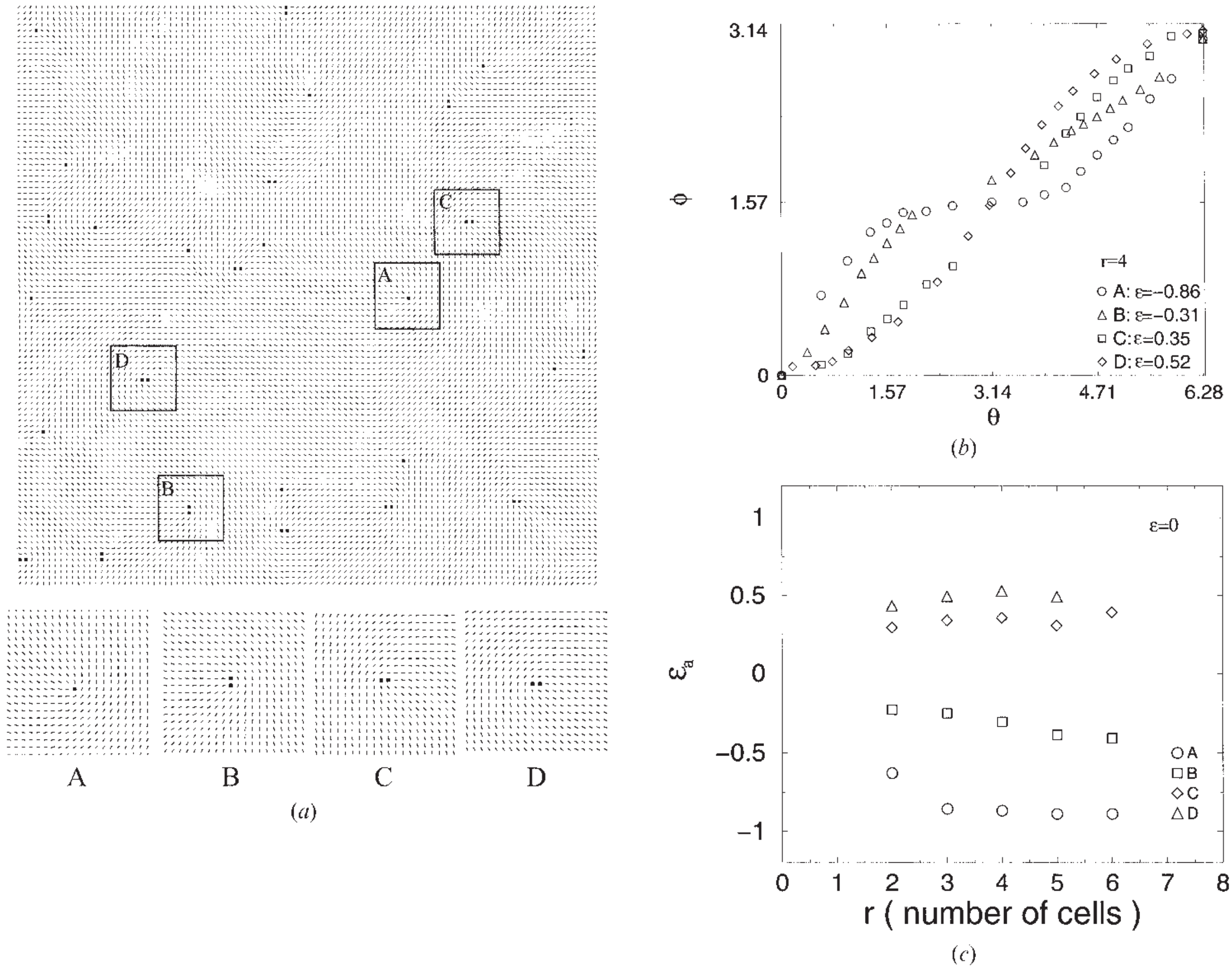

Figure 2. (*a*) The disclinations quenched at 300 time steps performed on a 100×100 lattice with equal elastic constants ($\varepsilon = 0$) and periodic boundary conditions. Small filled boxes represent the disclination cores. (*b*) The $\phi(\theta)$ data at $r = 4$ (the number of cells); (*c*) the results of $\varepsilon_a(r)$ measured from the four selected $+1/2$ disclinations A, B, C and D highlighted in (*a*).

symmetric as those obtained from single disclinations in figure 1 (*f*) because of the interaction of neighbouring disclinations. As a result, the values of ε_a fall in the range of -1 to 1, as shown in figure 2 (*c*). Obviously, the variation of the *apparent* elastic anisotropy is similar to that measured from the observed disclinations under the polarizing light microscope [1].

The assumption of equal elastic constants in fact makes the system free of the effect of elastic anisotropy. Therefore, only neighbouring disclinations could contribute to the different distortions of the $+1/2$ disclinations. This may be the reason why there are great variations in the *apparent* elastic anisotropy measured in experiment and simulation. Thus the impact of disclination interaction is not negligible. However, when the elastic constants are unequal, *i.e.* the effect of elastic anisotropy is turned on, how do the disclinations respond? Is the disclination interaction weak enough to be neglected, compared with the effect of strong elastic anisotropy?

3.2.2. *Splay–bend elastic anisotropy,* $k_{11} \neq k_{33}$

Simulations with $k_{11} \neq k_{33}$ show that disclination interaction still plays a significant role even though the system has strong elastic anisotropy. Theoretically, as the distinction between the splay and the bend constants is increased, the impact of elastic anisotropy on the structure of a $+1/2$ disclination emerges and gradually dominates, just as shown in figure 1 for the ideal single $+1/2$ disclinations. The tensor model is used to generate disclinations on the condition of unequal elastic constants in a polydomain system. The

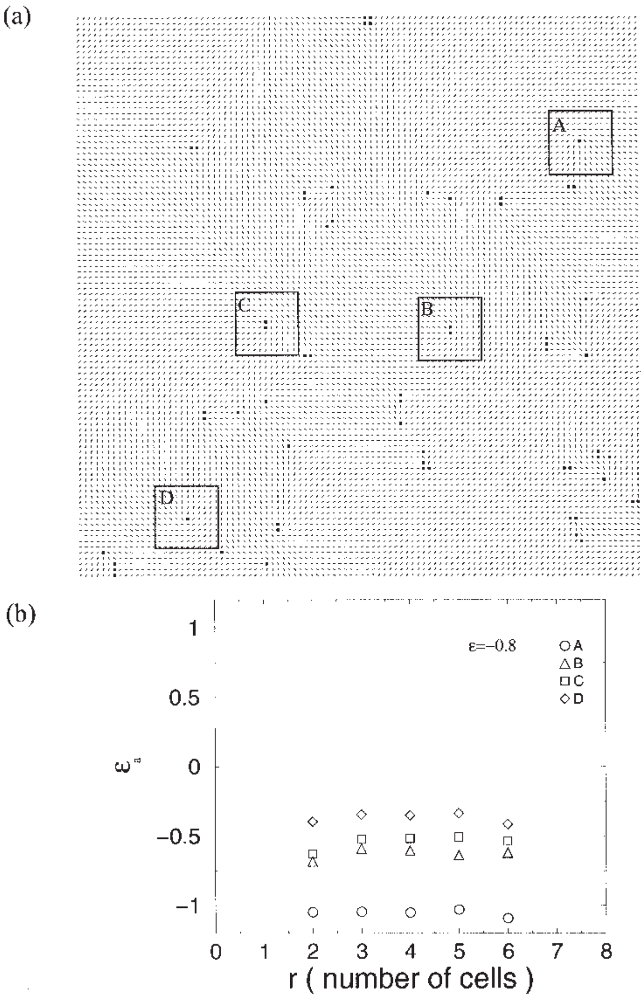

Figure 3. (*a*) The disclinations quenched at 800 time steps run on a 100×100 lattice with $10k_{11} = k_{33}$ ($\varepsilon \approx -0.8$) and periodic boundary conditions. Small filled boxes represent the disclination cores. (*b*) The results of $\varepsilon_a(r)$ measured from the four selected $+1/2$ disclinations A, B, C and D highlighted in (*a*).

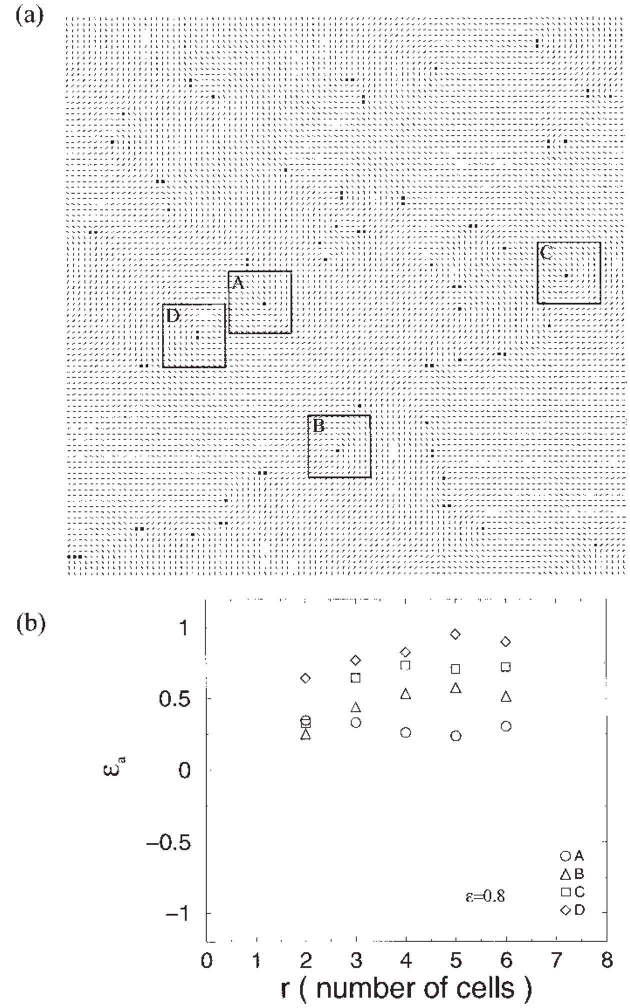

Figure 4. (*a*) The disclinations quenched at 800 time steps run on a 100×100 lattice with $k_{11} = 10k_{33}$ ($\varepsilon \approx 0.8$) and periodic boundary conditions. Small filled boxes represent the disclination cores. (*b*) The results of $\varepsilon_a(r)$ measured from the four selected $+1/2$ disclinations A, B, C and D highlighted in (*a*).

disclinations are also quenched after the density of disclinations has substantially decreased.

Figures 3 and 4 show snapshots of the director field and the $+1/2$ disclinations selected in the cases of $k_{11} = 10k_{33}$ and $10k_{11} = k_{33}$, *i.e.* $\varepsilon \approx -0.8$ and $\varepsilon \approx 0.8$, respectively. The obvious change of distortions around $+1/2$ disclinations can easily be spotted. The same method as before is used to measure the apparent elastic anisotropies from the $+1/2$ disclinations in these two cases with the strong elastic anisotropy. However, the data show a significant distribution about the predefined value of either $\varepsilon = -0.8$ or $\varepsilon = 0.8$. As a result, the values of the apparent elastic anisotropy in both cases are also in a range, as shown in figures 3 (*b*) and 4(*b*). It is unsurprising that the range shifts up, 3(*b*), or down, 4(*b*), to a relatively narrow region, when the splay constant is either much larger or much less than the bend constant, respectively. It is clear however that the interaction between neighbouring disclinations is still active in the presence of strong elastic anisotropy. The configuration of every disclination is a consequence of the balanced effect of both disclination interaction and intrinsic elastic anisotropy.

Despite the variation of ε_a, the mean of its distribution range seems to indicate the condition of elastic anisotropy of the system. The range $-1 \leqslant \varepsilon_a \leqslant 1$ may imply that the intrinsic clastic anisotropy ε is approximately zero, and $-1 \leqslant \varepsilon_a < 0$ or $0 < \varepsilon_a \leqslant 1$ may mean $\varepsilon < 0$ or $\varepsilon > 0$. Hence, comparing the results of ε_a measured above with the wide distribution of ε_a measured from the disclinations observed by optical microscopy (see [1]), Cl-6 copolyester is inferred to have approximately equal elastic constants. *i.e.* $\varepsilon \approx 0$ (the mean of ε_a by experimental measurements is -0.08, see [1]).

4. Effect of disclination interaction

The dramatic variation of distortions around the $+1/2$ disclinations in the same sample demonstrates the complicated interaction between multiple neighbouring disclinations. It is known that disclinations often group in pairs of opposite signs. There is no easy way to obtain a general analysis of the interaction if more than one defect is present. In the following discussion, pairs of $(+1/2, -1/2)$ disclinations in a system with equal elastic constants are studied in order to discriminate in more detail between disclination interaction and elastic anisotropy.

4.1. *Patterns of disclination pairs*

With equal elastic constants, an isolated $(+1/2, -1/2)$ disclination pair, $+1/2$ at (x_1, y_1) and $-1/2$ at (x_2, y_2) can be described by employing the superposition principle [10]:

$$\phi = \frac{1}{2}\tan^{-1}\frac{y-y_1}{x-x_1} + \frac{1}{2}\tan^{-1}\frac{y-y_2}{x-x_2} + c_0 \tag{8}$$

where c_0 determines the relative orientation between the two disclinations.

Imagine that a $-1/2$ disclination could be taken round a $+1/2$ disclination, as presented in figure 5. The

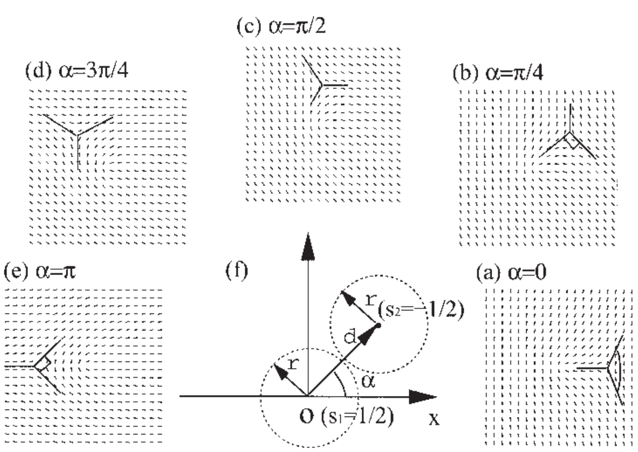

Figure 5. Five typical director patterns for $(+1/2, -1/2)$ disclination pairs in nematics. (*a*) and (*e*) are two extreme configurations of pairs, with the centre region showing either predominant splay or predominant bend. (*b*), (*c*) and (*d*) are the patterns between the extremes of (*a*) and (*e*). (*f*) The core of the disclination of $s_1 = +1/2$ is the origin, with its symmetric axis fixed along the x axis. The relative orientation and position of the neighbouring disclination $s_2 = -1/2$ is defined by the angle α.

core of the $+1/2$ disclination is chosen as the origin and its symmetric axis is fixed and parallel to the x axis. The relative position of the $-1/2$ disclination is defined by α, which is the angle between the central line of the pair and the x axis. The five typical patterns of disclination pairs are actually generated depending on c_0 in equation (8), and there is a simple linear relationship between α and c_0, $\alpha = \pi + 2c_0$. In the following discussion, α is used as the angle descriptor to define the angular position of the $-1/2$ disclination of the pair in relation to the other.

4.2. *Director fields around each of the defects of a (+1/2, −1/2) pair*

The energy analysis of all the pairs is performed on a 100×100 lattice by applying equation (2). The total energy of the pair means that the elastic free energy is contained in the region with a given radius $R \leqslant 48$, contributed by the splay and bend energies, as shown in figure 6 (*a*). Similarly, the total energy of an individual $+1/2$ or $-1/2$ disclination in the pair is the elastic free energy in the region from the core to the radius r. Here, the pair at $\alpha = 0$ is considered first, which is one of the two extreme patterns described by Ranganath [2]. Figure 6 (*b*) shows the energy profile of this pair as a function of the disclination separation d. The total energy of the pair is logarithmically proportional to the distance between the two defects, in good agreement with the analytical expression [10]. So disclination pairs attract each other and tend eventually to annihilate each other in order to minimize the total elastic free energy. Furthermore, the splay energy is higher than the bend energy as shown in figure 6 (*b*). In the assumption of equal elastic constants, this means that the splay distortion plays a dominant role in this type of pair, which supports Ranganath's proposal [2].

Figure 6 (*c*) shows the proportion of the splay and bend energies of the $+1/2$ disclination relative to its own total energy, as a function of the radius r in the pair at $\alpha = 0$ with the disclination separation $d = 10$, 15 or 25. To allow comparison with a disclination free of a neighbouring interaction, the splay and bend energies for a single $+1/2$ disclination in the case of equal constants, figure 1 (*c*), are also plotted in figure 6 (*c*). In this case, the splay and bend energy are equal. In figure 6 (*c*), the balance of the splay and bend energies for the $+1/2$ disclinations is interrupted by the $-1/2$ disclination neighbour, through increasing the splay distortions and decreasing the bend distortions. Moreover, the difference between the splay and bend energies increases as the radius is increased at the interval (0, $d/2$). When the radius is increased further, such as $r > d/2$, the interaction becomes more complicated since

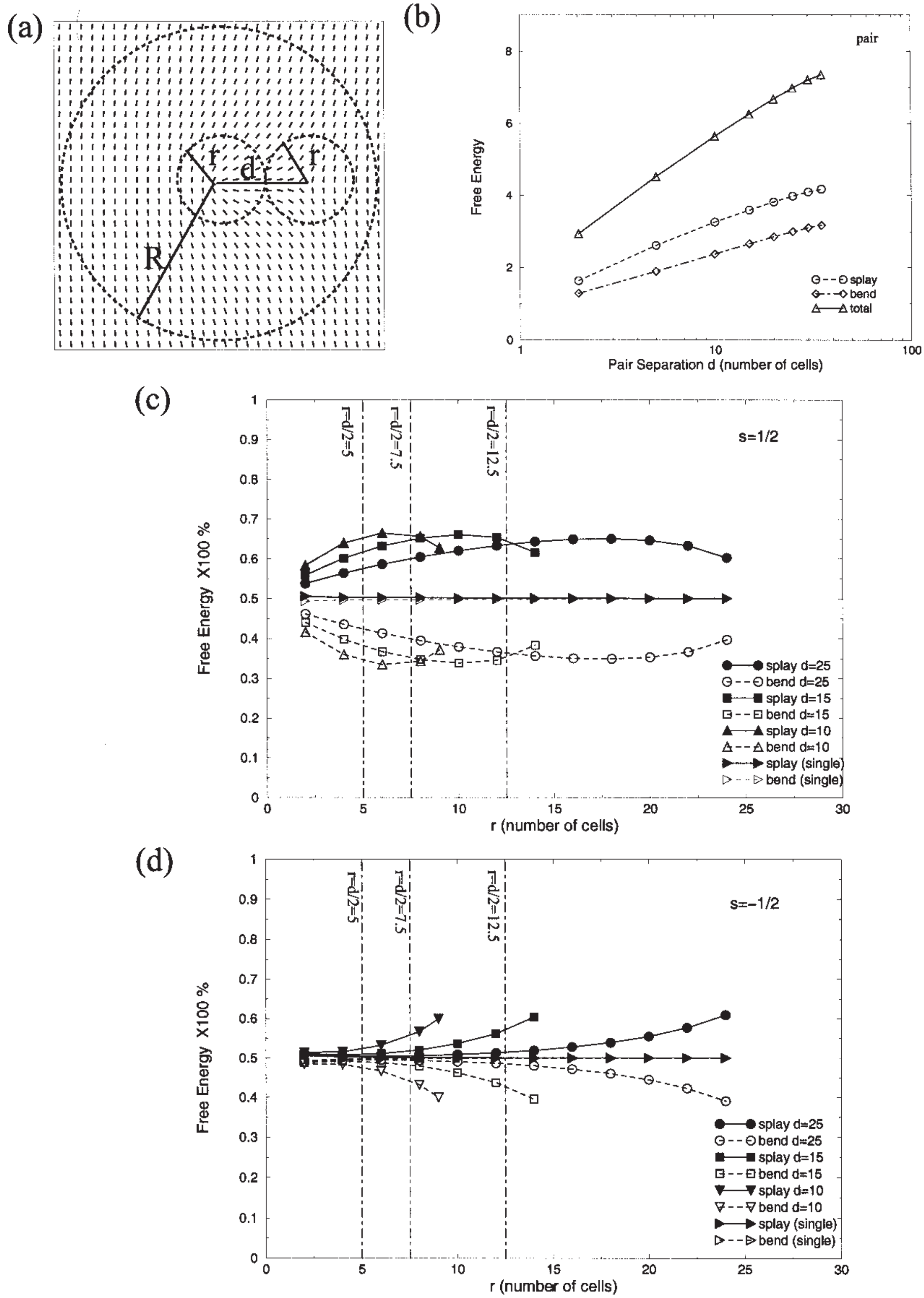

Figure 6. (*a*) The disclination pair (+1/2, −1/2) at $\alpha = 0$. (*b*) The total, splay and bend energies of the pair as a function of the disclination separation, *d*. (*c*) The proportion of the splay and bend energies of the +1/2 disclination relative to its own total energy, as a function of the radius *r* from its core, the proportion being calculated for different separations $d = 10$, 15 and 25. (*d*) The proportion of the splay and bend energies of the −1/2 disclination relative to its own total energy as a function of the radius, the proportion being calculated for different separations $d = 10$, 15 and 25.

more distortions induced by the $-1/2$ disclination are involved. When considering the distance between the two defects, the energy curves seem to converge into the narrow regions as the distance d is decreased. As a result, the closer the two defects are, the larger is the distinction between the splay and bend energies at a given radius. This has been interpreted analytically as an interaction force which is inversely proportional to the separation [10]. Due to the relative scale of the lattice, increasing the distance of the pair can be viewed as increasing the resolution of the director field surrounding the defect cores of fixed separation. figure 6 (*c*) shows that the difference between the splay and bend energies for a $+1/2$ disclination induced by a neighbouring $-1/2$ disclination cannot be ignored, in spite of large separation or high resolution. However, the diagrams indicate that the value of $\varepsilon_a(r)$ will turn to the intrinsic anisotropy for measurements made closer to the core than 10% of the separation of the pair.

Figure 6 (*d*) shows the proportion of the splay and bend energies of the $-1/2$ disclination relative to its own total energy, as a function of the radius r in the pair at $\alpha = 0$ with the disclination separation $d = 10$, 15 or 25. Clearly, the $+1/2$ and $-1/2$ disclinations show very different energy profiles. For the $-1/2$ disclinations in figure 6 (*d*), the splay and bend energies are almost equal in the region of $r < d/2$. The difference between the splay and bend energies grows gradually if $r > d/2$ and more distortions induced by the neighbouring $+1/2$ disclination are involved. Similar energy profiles are shown with the different separations.

Therefore, the splay and bend distortions for the $-1/2$ disclination are insensitive to its $+1/2$ disclination neighbour. Of course, the anisotropy of the director field around a $-1/2$ disclination is insensitive to the intrinsic anisotropy either [2]. It is the $+1/2$ disclination that contributes most to the distinction between the splay and the bend energies of the pairs.

4.3. *Interaction and patterns of disclination pairs*

With $\alpha = \pi$, the disclination pair in figure 5 (*e*) shows another extreme pattern, with the dominant bend distortions in the intervening field between the two disclinations, also as described by Ranganath [2]. The energy profiles for this pattern are exactly the same as those in figure 6 if the data for the splay and bend energies are exchanged. For the other patterns of disclination pairs at $0 < \alpha < \pi$, the difference between the splay and bend energies changes continuously with α. Figure 7 shows how the distribution of the splay and bend energies varies with the relative orientation of the two disclinations with the separation $d = 25$. The total energy and the energies attributable to the splay and bend distortions of the pairs are shown as a function of α in figure 7 (*a*). It is interesting that the total energy of all types of pairs is fairly constant. Therefore, there is no energy involved when taking a $-1/2$ disclination round a $+1/2$ disclination, *i.e.* the probability for any given disclination pair is equal in the condition of equal

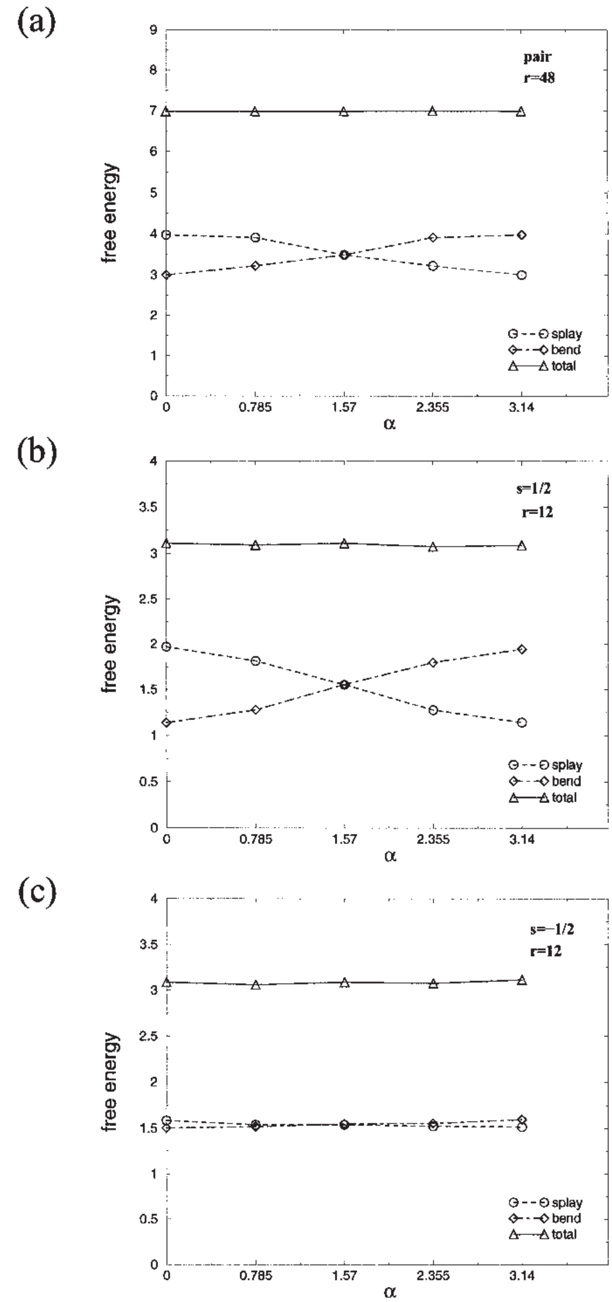

Figure 7. (*a*) The total, splay and bend energies of $(+1/2, -1/2)$ pairs *versus* the relative orientation α of the $-1/2$ disclination. (*b*) The variation of the total, splay and bend energies of the $+1/2$ disclination of the pair with α. (*c*) The total, splay and bend energies of the $-1/2$ disclination of the pair as a function of α.

constants. Furthermore, the splay energy of the pairs decreases while the bend energy increases as α changes from 0 to π. The difference between the splay and bend distortions reaches a maximum at $\alpha=0$ or π.

Figures 7 (*b*) and 7(*c*) show the total energy and the energies attributable to the splay and the bend distortions of the $+1/2$ and $-1/2$ disclinations in the pairs as a function of their relative orientation. The energy curves for $+1/2$ disclination in figure 7 (*b*) have similar profiles to those for the whole pairs in figure 7 (*a*). However, for the $-1/2$ disclination, the proportion of the splay and bend energies is almost equal, as shown in figure 7 (*c*). All these energy profiles may demonstrate why there are the great variations of *apparent* elastic anisotropy in the polydomain systems in the case of equal elastic constants.

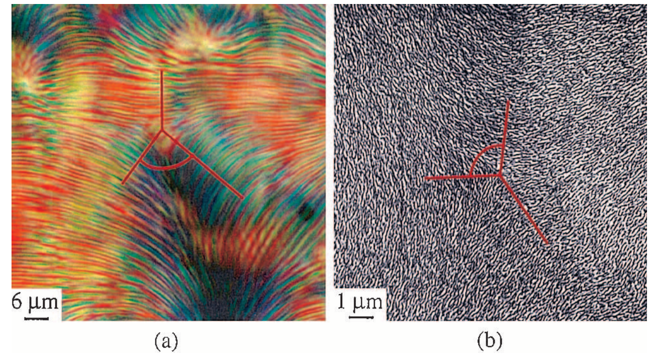

Figure 8. (*a*) Optical micrograph of a $-1/2$ disclination revealed by spontaneous band texture in the nematic phase of the semi-rigid Cl-6 copolyester. (*b*) SEM micrograph of a $-1/2$ disclination decorated by lamellar structure in the nematic phase of the random rigid BN(1:1) copolyester.

4.4. *Discussion*

It is clear that the splay and bend distortions around $+1/2$ disclinations are sensitive to disclination interaction. By contrast, the splay and bend distortions of $-1/2$ disclinations are remarkably insensitive to neighbouring interaction. These results seem reminiscent of the relationship between the $+1/2$ and $-1/2$ disclination structures and elastic anisotropy. However, the puzzle is how the $-1/2$ disclination can remain unchangeable in the presence of a disclination interaction. Interestingly, a close examination of the $-1/2$ disclinations shows that the threefold structure for the $-1/2$ disclination is no longer fully symmetrical in some types of pairs. For instance in figure 5 (*e*), for the $-1/2$ disclination in the pair at $\alpha=\pi$, one angle between its two symmetric axes is narrowed from $2\pi/3$ to around $\pi/2$ so that more bend and fewer splay distortions associated with the neighbouring $+1/2$ disclination emerge in this region. Consequently, the other two neighbouring angles become wider and spread to $3\pi/4$ respectively, and hence more splay and less bend distortions are created. More cases can be found in figures 5 (*a*) and 5(*b*). By adjusting the three angles between its symmetric axes, the $-1/2$ disclination keeps the splay and the bend elastic energies almost unchanged. In fact, the symmetry of the $+1/2$ disclinations is also challenged, except for the two extreme patterns of pairs with $\alpha=0$ and π. In many cases, the $+1/2$ disclinations still maintain their symmetry, but the symmetry is not perfect, as shown the distortion data $\phi(\theta)$ in figure 2 (*b*).

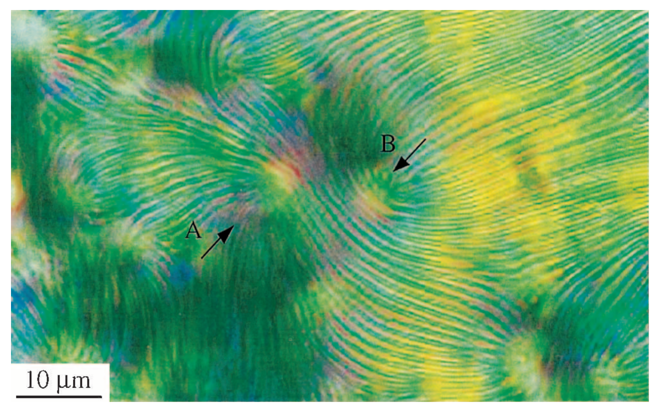

Figure 9. A group of disclinations revealed by spontaneous band texture in the nematic phase of Cl-6 copolyester. Two neighbouring $+1/2$ disclinations show considerably different distortions.

4.5. *Further experimental observation*

There are convincing experimental observations revealing the deformed structure of the disclinations. Part I [1] presented a few $+1/2$ disclinations in a full range of configurations, from 'sunrise' to 'archway'. Figure 8 (*a*) shows the deformed structure of a $-1/2$ disclination revealed by spontaneous band texture in the semi-rigid Cl-6 copolymer under a polarizing light microscope. It can be seen that, for the $-1/2$ disclination, the three angles between its symmetric axes are unequal. Figure 8 (*b*) shows similar deformed structures of a $-1/2$ disclination revealed by lamellar structure in the rigid BN(1:1) copolymer [11] under a scanning electron microscope (SEM). The morphology of the $-1/2$ disclinations at a higher resolution indicates that the change of the structure starts near the core. Unfortunately, as mentioned before, exploring the structure closer the core is beyond the optical method where the disclinations of the array are less than a few 10s of microns apart.

The real situation is more complex because one defect always has more than one neighbour. Typically, there are 2 ~ 6 surrounding disclinations. Figure 9 gives an example of a cluster of disclinations as revealed by band texture. There are more than two disclinations surrounding each disclination, including both −1/2 and +1/2 disclinations. The structure of an individual disclination is the result of a competition between attractive and repulsive forces with multi-neighbours. Therefore, disclinations with various configurations emerge simultaneously, such as the +1/2 disclination A and B in figure 9 showing two distinct configurations. Furthermore, during the evolution of the texture, the disclination interaction varies with the disclination density. It is conceivable that the structures of +1/2 and −1/2 disclinations would continuously change during the whole evolution of the texture.

5. Conclusions with summary

The combination of the experimental measurements with the numerical simulation demonstrates that the structures of disclinations are the result of competition between disclination interaction and elastic anisotropy during the texture evolution. The conclusions may be summarized thus:

(1) The measurements of the distortion field around selected +1/2 disclinations by an optical method show a distortion, expressed in term of ε_a, which is constant over a significant radius range, *r*/*d* from 0.05 to 0.5 (*d* the disclination seperation). This radius range is accessible by the optical (band texture decoration) technique used.

(2) The measured values of ε_a vary widely for different +1/2 disclinations selected. This wide variation has been shown to be the result of interaction with neighbouring disclinations.

(3) Simulation by the tensorial lattice model confirms that the wide variations of ε_a is due to the influence of neighbouring disclinations, but that the range will be distributed about a value of ε, characteristic of the intrinsic anisotropy of the liquid crystal.

(4) The measurement of elastic anisotropy obtained on the basis of the continuum theory by measuring the distortion of any single wedge disclination should only be used if the disclination is isolated. Practically, the measurement of the intrinsic anisotropy will require that the distance of the disclination to the nearest neighbours is larger than the distance from its core at which the anisotropy is measured (at $r/d < 0.05$) or averages of the apparent anisotropies from a wide range of +1/2 disclinations, or, ideally, a combination of both.

(5) It would appear that the value of intrinsic anisotropy of the main chain polymer examined, Cl-6, which has flexible spacers $(CH_2)_6$ in its backbone is close to zero. This result suggests the role of hairpin in compensating for density gradients under splay distortion.

(6) The simulation results suggest that disclination interaction has a considerable effect on the structures of both +1/2 and −1/2 wedge disclinations. The distortion of a +1/2 disclination depends not only on elastic anisotropy, but also on the disclination interaction. The splay and bend distortions around the +1/2 disclination vary with the relative orientation of its neighbouring −1/2 disclination. A −1/2 disclination adapts itself in polydomains by changing the angles between its three symmetric axes. The elastic free energies attributable to the splay and bend distortions around the −1/2 disclination remain almost constant and are sensitive to neither the elastic anisotropy nor the neighbouring disclinations.

W. S. would like to acknowledge the support of an Overseas Research Student (ORS) Scholarship, a Cambridge Overseas Trust Scholarship, and the Department of Materials Science and Metallurgy, University of Cambridge. Support by the EPSRC grant under its 'processing of conventional structural materials' program is appreciated.

References

[1] SONG, W., FAN, X., WINDLE, A. H., CHEN, S., and QIAN, R., 2003, *Liq. Cryst*., **30,** 7.
[2] RANGANATH, G. S., 1983, *Mol. Cryst. Liq. Cryst.*, **97,** 77.
[3] BEDFORD, S. E., NICHOLSON, T. M., and WINDLE, A. H., 1991, *Liq. Cryst.*, **10,** 63.
[4] ZAPOTOCKY, M., GOLDBART, P. M., and GOLDENFELD, N., 1995, *Phys. Rev. E*, **51,** 1216.
[5] HOBDELL, J. R., and WINDLE, A. H., 1997, *Liq. Cryst.*, **23,** 157.
[6] TU, H., GOLDBECK-WOOD, G., and WINDLE, A. H., 2001, *Phys. Rev. E*, **64,** 1704.
[7] TU, H., GOLDBECK-WOOD, G., and WINDLE, A. H., 2002, *Liq. Cryst.*, **29,** 325.
[8] TU, H., GOLDBECK-WOOD, G., and WINDLE, A. H., 2002, *Liq. Cryst.*, **29,** 335.
[9] WANG, W., HASHIMOTO, T., LIESER, G., and WEGNER, G., 1994, *J. Polym. Phys.*, **32,** 2171.
[10] NEHRING, J., and SAUPE, A., 1972, *J. Chem. Soc.: Faraday Trans. II*, **68,** 1.
[11] WILSON, D. J., VONK, C. G., and WINDLE, A. H., 1993, *Polymer*, **34,** 227.